A Study of Unidirectional Versus Tridirectional Heat Flux Models and the Effect of Particle Size on Heat Conduction in Composite Solids

THOMAS P. FIDELLE, JR. and R. S. KIRK

Chemical Engineering Department
University of Massachusetts, Amherst, Massachusetts 01002

The effect of the assumption of unidirectional heat flux was determined for a well-known unit cell model used to predict effective thermal conductivities of particulate composites. Predictions obtained for the condition of unidirectional heat flux were compared with those obtained for the more rigorous case of tridirectional heat flux. The latter case required a digital simulation of the model to obtain three-dimensional temperature distributions. Comparisons were made for two different values of pure component thermal conductivity ratio and for a broad range of phase compositions. Results in each case suggest that the unidirectional heat flux assumption is not a serious limitation.

Experimental studies were made of the effects of composition, particle size, and pure component thermal properties on the effective thermal conductivity of three different composite systems. Cylindrical samples of each system were cast from various proportions of their basic constituents. Effective thermal conductivities were calculated from effective thermal diffusivities. The latter were obtained experimentally from the thermal response of the center of each composite sample as it was cooled from room temperature to 0°C. by means of an agitated ice bath. Effective conductivities so obtained were compared with conductivities predicted by the tridirectional simulation and three previously published models. Results show that a recent model that utilizes unidirectional heat flux but permits random phase distribution provides the best predictions of the experimental data presented in this work.

Results of the particle size study indicate that there is a minimum ratio of system dimension to particle dimension below which a particulate composite can no longer be considered macroscopically homogeneous and isotropic.

A popular technique for predicting effective thermal conductivities of particulate composites employs a unit cell to characterize the heat conductivity of the macrostructure. For mathematical simplicity, it is customary to assume unidirectional heat flux in the unit cell; then the cell resistance is simply the resultant of a network of smaller resistances in series and parallel.

In this work thermal conductivity of a unit cell is calculated on the basis of tridirectional heat flux. Results are compared with conductivities predicted by a well-known model assuming unidirectional heat flux. The comparison shows that the assumption is not severely limiting.

In addition, some new experimental data on composite systems are reported and compared with the more recent models for predicting effective thermal conductivities. A model by Cheng and Vachon (*1*) furnishes the best predictions.

Only particulate composites are considered in this study. Such systems have readily distinguishable continuous and dispersed phases, often called matrix and filler, respectively. Thermal conductivity values for large samples of particulate composites are independent of sample size and of the direction of the applied thermal gradient if the filler particles are small and well-distributed in the matrix. Such systems are said to be macroscopically homogeneous and isotropic; what one really observes is bulk, or effective thermal conductivity.

It was found that there is a critical ratio of system dimension to particle dimension below which a composite system can no longer be considered macroscopically homogeneous and isotropic.

BACKGROUND

The literature abounds in models for predicting effective thermal conductivities of particulate composites. Some of the more recent examples will be mentioned here. Explicit expressions, where applicable, are listed in Table 1. A number of excellent review articles (*2* to *4*) give additional information on available models.

Many models utilize the concept of a basic element of the composite, which consists of a particle of the dispersed phase surrounded by material of the continuous phase. The thermal conductivity of the element is calculated and reported as the effective thermal conductivity of the composite system.

Two different methods are used to relate the basic element to its macrostructure. The more common unit cell method assumes that the basic element is one of many identical cubes stacked in a cubic array to form the composite system. The other method, called the self-consistent scheme, assumes that the basic element is embedded in a fictitious homogeneous medium, whose thermal conductivity is the unknown effective thermal conductivity of the composite.

Thomas P. Fidelle, Jr., is at Fiber Industries, Inc., Charlotte, North Carolina.

Table 1. Explicit Expressions for Predicting Effective Thermal Conductivities of Particulate Composites

Expression	Source
$(\phi - 1)\dfrac{k^I - k_{\text{eff}}}{k^I + 2k_{\text{eff}}} = \phi\dfrac{k^{II} - k_{\text{eff}}}{k^{II} + 2k_{\text{eff}}}$	Landauer (8)
$\dfrac{k_{\text{eff}}}{k^I} = \dfrac{2k^I + k^{II} - 2\phi(k^I - k^{II})}{2k^I + k^{II} + \phi(k^I - k^{II})}$	Maxwell (9)
$k_{\text{eff}} = \dfrac{1}{\displaystyle\int \dfrac{dP_1}{k^I + (k^{II} - k^I)\displaystyle\int \dfrac{1}{\sigma\sqrt{2\pi}} e^{-0.5\left(\frac{P_1 - \mu}{\sigma}\right)^2} dP_1}}$	Tsao (12)
$\dfrac{1}{k_{\text{eff}}} = \dfrac{1 - B}{k^I} + \dfrac{B^{0.5}}{2\{(k^{II} - k^I)\,[k^I + B(k^{II} - k^I)]\}^{0.5}} \ln \dfrac{\{k^I + B(k^{II} - k^I)\}^{0.5} + \{B(k^{II} - k^I)\}^{0.5}}{\{k^I + B(k^{II} - k^I)\}^{0.5} - \{B(k^{II} - k^I)\}^{0.5}}$ $B = \sqrt{1.5\phi}$ $k^{II} >> k^I$	Cheng and Vachon (1)
$\dfrac{k_{\text{eff}}}{k^I} = 1 - 1.21\phi^{0.67} + 0.4875\phi^{0.33}\left[\dfrac{\ln\frac{k^{II}}{k^I} - 1}{0.25 + (0.403\phi^{-0.33} - 0.5)\left(\ln\frac{k^{II}}{k^I} - 1\right)}\right]$	Jefferson (18)

In the unit cell method, it is customary to designate a principal direction of heat transfer (PDHT) and to assume that heat flux is unidirectional, that is, there are no flux components normal to the PDHT. This also means that planes perpendicular to the PDHT are isothermal. That being the case, the effective resistivity of the cell is simply the resultant of a network of smaller resistances in series and parallel.

Prior evidence suggests that the assumption of unidirectional heat transfer is not very restrictive. Deissler and Eian (5), for instance, studied the effective thermal conductivities of granular solids. They used a numerical relaxation procedure to obtain the two-dimensional temperature distribution in a unit cell derived from a rectangular array of long cylinders. Krupiczka (6) obtained an analytical solution for the same cell. Both investigators extended their results, by approximation, to the case of a cubic array of spheres in point contact with one another. Deissler found no improvement over simpler, unidirectional models when the new results were compared with existing experimental data. However, the lack of improvement could be due to the approximations made in extending the solutions to the three-dimensional case.

Hashin (7) analyzed the self-consistent scheme method, which does not depend upon the assumption of unidirectional heat flux. However, there is some question as to what constitutes the basic element. Hashin showed how two different expressions for effective thermal conductivity, developed previously and independently, could be obtained by using two different configurations of the basic element. One expression, attributed to Landauer (8), is applicable to granular composites, such as powders and packed beds. The other, originally developed by Maxwell (9), is reputed to be one of the better predictors for dispersed composites (2, 10).

The few models that avoid the concept of a basic element rely on some probabilistic distribution of species. Baxley and co-workers (11) proposed a digital simulation technique for predicting effective thermal conductivities of two-phase systems. A random number generator governs the distribution of cubes of the filler phase among cubes of the matrix phase to form the composite system, a large cubic array of the smaller cubes. A thermal gradient is established between two opposite faces of the system, and the remaining faces are insulated. The three-dimensional temperature distribution, based on the steady state requirement of no accumulation of energy in the system, is then obtained by a systematic relaxation technique. Average heat flux and average (that is, effective) thermal conductivity are obtained from the resultant temperature distribution. The model affords no explicit relationship for predicting effective thermal conductivities.

Tsao (12) proposed a technique that avoids the basic element concept but retains the assumption of unidirectional flux. The model, consisting of irregularly shaped particles in complete disorder in a matrix, is sliced into thin sections perpendicular to the PDHT. The filler within each slice is rearranged to occupy a rectangular area at the bottom of the slice. The slices themselves are rearranged in order of decreasing filler concentration. The unidirectional heat flux assumption justifies these rearrangements. The net effect is a simpler system whose conductivity equations are tractable. Tsao suggested the normal distribution function to describe the concentration profile. This requires two parameters, the mean and variance of filler concentration. If the sample is large enough, the former is simply the filler volume fraction. The latter, however, must be estimated or measured directly by some sampling technique. Warren and Messmer (13) criticized this approach on the basis that the use of a stochastic model implies the assumption that the behavior of the system is governed solely by its bulk properties. Cheng and Vachon (1) approximated the normal distribution function by a parabolic profile, thereby eliminating the additional parameter.

The unit cell models specify some ideal shape of filler particle, such as sphere, ellipsoid, etc. This is not a serious restriction because particles of real fillers often approach spheres. Nielson (14) contends that discrepancies between experimental and theoretical results are caused by factors other than small deviations from spherical shape. Conversely, large deviations from spherical shape have a considerable effect on heat conductivity, as shown by Hamilton and Crosser (15), who studied cylinders and discs as well as spheres. They introduced an empirical factor into Maxwell's expression to account for deviations from spherical shape. An additional complication with nonspherical particles lies in their lack of symmetry about a point; any bias in orientation with respect to the boundaries of the

system will lead to anisotropic behavior. Some theoretical work has been done on nonspherical particles (*16, 17*).

None of the models known to us explicitly accounts for particle size. Rather they envision some hypothetical test specimen which is much larger than a typical particle. On this qualitative condition, the system is said to be macroscopically homogeneous and isotropic, and particle size is immaterial. Experimentally, using spherical particles, Hamilton and Crosser found little effect of particle diameter on effective thermal conductivity for a 100-fold change in the diameter.

MODEL DEVELOPMENT

Effect of Unidirectional Heat Flux

One way to determine the legitimacy of the unidirectional heat flux assumption is to compare, for the same geometric model, effective thermal conductivities obtained alternately with and without this simplifying assumption. If the differences are great, the assumption is not realistic. Deissler and Eian (*5*) and Krupiczka (*6*) took this approach. However, they considered bidirectional heat flux, which is still short of the true physical picture of tridirectional flux. The present work considers tridirectional flux, which, due to the complexity of the equations involved, requires a numerical solution technique adaptable to machine computation.

A unit cell model first proposed by Jefferson et al. (*18*) was used for the present study. The model consists of a sphere of the filler phase concentric with a cube of the matrix phase. It was chosen because it aptly describes most real particulate fillers, which are spherical or nearly so (*14*). The original authors assumed unidirectional heat flux and derived an explicit expression for effective thermal conductivity (Table 1).

Because of symmetry, only one-eighth of the unit cell requires consideration (Figure 1). Laplace's equation governs the steady state temperature distribution in each phase. For constant thermal conductivity

$$\nabla^2 T^i = 0; \quad i = I, II \tag{1}$$

The following boundary conditions are either specified or implied by symmetry:

$$T^I = \tau_1; \qquad z = 1 \tag{2}$$

$$T^i = \tau_2; \qquad i = I, II; \qquad z = 0 \tag{3}$$

$$\frac{dT^i}{dn} = 0; \quad \begin{cases} i = I, II; & x = 0 \\ i = I, II; & y = 0 \\ i = I\ \ ; & x = 1 \\ i = I\ \ ; & y = 1 \end{cases} \tag{4}$$

where all variables are normalized and dimensionless, and d/dn denotes the directional derivative normal to a surface or interface. Matching conditions at the phase interface, assuming no contact resistance, are

$$\left.\begin{aligned} T^I &= T^{II} \\ \frac{dT^I}{dn} &= \theta \frac{dT^{II}}{dn} \\ \theta &= \frac{k^{II}}{k^I} \\ c &= \left(\frac{3\phi}{4\pi}\right)^{1/3} \end{aligned}\right\} x^2 + y^2 + z^2 = c^2 \tag{5}$$

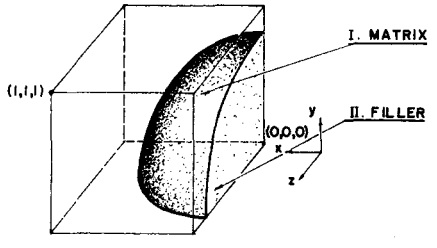

Fig. 1. One-eighth of the Jefferson unit cell.

Simulation of a Unit Cell

The solution of Equations (5) will yield the calculated temperature distribution resulting from tridirectional heat flux. This was accomplished for the system of Figure 1 by simulating the system in a digital computer program and solving Equations (1) through (5) in their finite-difference form.

The simulation consists of a rectangular array of nodes. To each node one assigns a temperature, according to some initial guess, and an algebraic sign, according to whether the node lies in the matrix (+) or filler (−) phases. This latter step establishes the phase interface, which is not a spherical surface, but the best approximation of one obtainable by a rectangular array of nodes. Specifically, if a node lies within the imaginary phase boundary, then so does its entire domain. The domain of a node is the mesh-size cube having the node at its center.

This approximate phase boundary makes the system very adaptable to machine computation but deviates from the assumed sphere. However, the denser the grid, the better the approximation. Accordingly, we gradually increased the grid density until we observed no differences in effective conductivity values of successively denser grids. This occurred for grids in the vicinity of 12 nodes square.

The final temperature distribution is obtained by an iterative relaxation technique similar to that used by Baxley et al. (*11*). One important difference is that Baxley's technique requires two locations of computer memory for each node, one each for the numerical values of temperature and pure component thermal conductivity. By using the dual logic of algebraic sign, our technique requires only one location of memory for each node, which effectively doubles the maximum possible array for a given capacity of memory.

The basic iterative expression for the j^{th} node is

$$T_j^* = T_j + \frac{w}{\sum_{p=1}^{6} k_p} \sum_{p=1}^{6} [k_p (T_p - T_j)] \tag{6}$$

where w is a relaxation factor between 1.0 and 1.8. The summation comes from the finite-difference form of Laplace's equation and the k_p depend upon the relationship between T_j and its six adjacent nodes.

$$k_p = 0; \qquad T_p \text{ lies on a no-flux surface} \tag{7}$$

$$k_p = k^I; \qquad T_p \text{ and } T_j \text{ both positive} \tag{8}$$

$$k_p = k^{II}; \qquad T_p \text{ and } T_j \text{ both negative} \tag{9}$$

$$k_p = \frac{k^I k^{II}}{2(k^I + k^{II})}; \qquad T_p \text{ and } T_j \text{ opposite in sign} \tag{10}$$

Equation (10) is an exact expression for the effective ther-

mal conductivity of a system of two dissimilar cubes in series (*19*).

The system is said to have converged to the desired temperature distribution when, for two successive iterations

$$\sum_j |T_j^* - T_j| \leq 0.1 \qquad (11)$$

Ideally the summation above should be identically zero, but 0.1 was found to be acceptable for practical purposes.

Average heat flux and effective thermal conductivity are determined from the model as follows: Between any two adjacent xy planes, the average minus z component of heat flux is given by

$$\bar{q} = -\frac{1}{M^2} \sum_x \sum_y [k_p (T(x, y, z) - T_p)] \qquad (12)$$

Effective, or average, thermal conductivity is simply the ratio of average heat flux to overall temperature gradient.

$$k_{\text{eff}} = \frac{\bar{q}}{-\frac{\Delta T}{\Delta z}} \qquad (13)$$

By substituting Equation (12) into Equation (13), one obtains

$$k_{\text{eff}} = \frac{\sum_x \sum_y [k_p(T(x, y, z) - T_p)]}{M^2 \frac{\Delta T}{\Delta z}} \qquad (14)$$

A meaningful check on convergence is the requirement that k_{eff} not vary significantly over the entire range of pairs of adjacent xy planes. With the convergence criterion of Equation (11), we found no change in the third significant figure of k_{eff}/k^I for successive xy plane calculations. This was considered acceptable.

By the foregoing procedure we obtained effective thermal conductivities versus filler fraction for several values of θ as the third parameter. These data were compared with conductivities predicted by the explicit expression of Jefferson (Table 1). Results for two values of θ are plotted in Figure 2. For small values of θ, Jefferson's model predicts conductivities consistently lower than those of the simulator. Differences between them increase slightly with increasing filler concentration, but the difference is less than 12% even at the relatively high concentration of 40%. For larger values of θ (for example, 1,000) Jefferson's model is biased lower than the simulator at lower concentrations and higher at higher concentrations. But even for this extreme case of θ the difference at 40% filler concentration is only 15%.

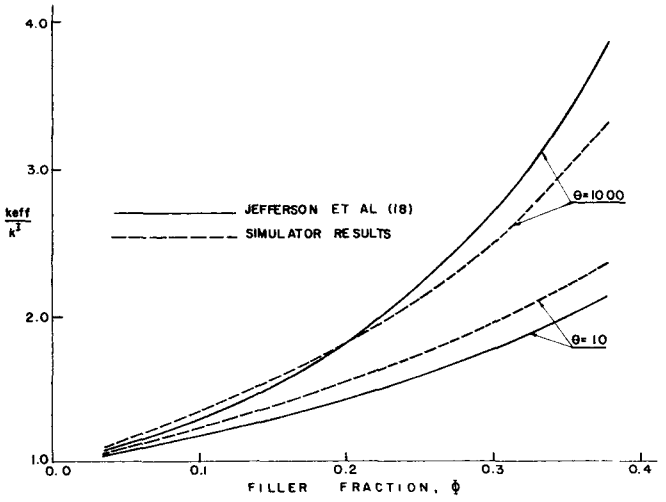

Fig. 2. Dimensionless effective thermal conductivity versus phase fraction for the Jefferson unit cell with and without the assumption of unidirectional heat flux.

There is some error in the simulator due to its departure from an ideally spherical interface. However, if this was the only source of discrepancy in Figure 2, one would expect a bias consistent in sign for all θ and decreasing in magnitude for increasing filler fraction.

The results of Figure 2 reinforce the conclusion of Deissler and Eian (*5*), that the unidirectional heat flux assumption is not a serious limitation. Considering the small differences involved, the unidirectional approach would appear to be preferable to the more complex tridirectional simulation which does not permit a simple, explicit expression for effective thermal conductivity.

EXPERIMENT

Scope

Experimental thermal conductivity data are presented for three different composite-solid systems covering a broad range of filler concentration and pure component thermal conductivity ratio. The data permit a comprehensive evaluation of the various models for predicting effective thermal conductivity. One of the three systems was also selected for a separate study of the influence of particle size on macroscopic homogeneity and isotropy.

Effective thermal conductivities reported in this work were calculated from experimentally determined effective thermal diffusivities and pure component heat capacities. Thermal diffusivities were obtained using a transient method: the thermal response at the center of a cylindrical test specimen being cooled from room temperature to 0°C. by means of an agitated ice bath. Diffusivity values were determined from the temperature-time data using a theoretical equation applicable to the experimental system. The transient technique was chosen for its simplicity, speed, and modest equipment demands. Heat capacities were measured against a sapphire standard in a differential scanning calorimeter.

After an extensive search for suitable systems—considering adaptability to mixing, casting, and curing without excessive air entrainment and/or particle settlement—we chose the following basic constituents: polyester resin and slow-curing plaster as matrices, and granular alumina, tabular alumina, and granular carborundum as fillers. Commercial sources of the materials are listed in Table 2 along with pure component properties and particle sizes. Except for the thermal conductivity of granular carborundum, consistent pure component properties were obtainable from manufacturers' literature, from published sources, or by direct measurement (cf. Table 2). Reported thermal conductivities for solid carborundum grains ranged from 110 to 133 B.t.u./(hr.)(ft.)(°F.) (*23*). As will be shown later, precise values of k^{II} for carborundum are unnecessary because the various models for predicting k_{eff} are insensitive to k^{II} at high values of θ. Therefore the mean value of 121 was used.

For each of the following systems, several cylindrical samples were cast in phase compositions ranging between 5 and 40% filler by volume: granular carborundum:plaster, granular alumina:plaster, tabular alumina:polyester.

The effect of particle size was studied on the carborundum-plaster system using four particle size ranges: −4+6, −8+10, −12+16, and −16+24 Tyler mesh. Samples containing 10 and 30% filler (by volume) were prepared from each fraction. The independent variable of interest is not particle size itself, but a term which relates the size of the test specimen to the

TABLE 2. PURE COMPONENT THERMOPHYSICAL PROPERTIES

Constituent	Source	Tyler mesh size range	Density, lb./cu.ft.	Heat capacity B.t.u./(lb.) (°F.)	Thermal conductivity, B.t.u./(hr.) (ft.) (°F.)
Plaster (cast)	U.S. Gypsum Spackling Putty	——	71.7	0.224‡	0.194**
Polyester (cast) KOPLAC 1082-3	Koppers Co., Inc.	——	72.4	0.274‡	0.094**
Resin Accelerator MEK peroxide	Wallace & Tiernan Inc.	——	——	——	——
Fused alumina grain	Norton Co.	−12 + 16	227.2*	0.178‡	22.5#
Carborundum grain	Norton Co.	−4 + 24	197.3*	0.150‡	121#
Tabular alumina	ALCOA	325	232.1†	0.178‡	22#

* Measured directly by displacement of water.
† Furnished by manufacturer.
‡ Measured directly in differential scanning calorimeter.
** Obtained from direct measurement of thermal diffusivity of pure cylindrical sample.
# See reference 23.

size of the particle. We arbitrarily chose the system dimension coincident with the PDHT, that is, the cylinder radius, and the apparent particle diameter as characterized by the sieve opening of the intermediate screen of the particle size range (for example, No. 9 mesh for the −8+10 fraction). Thus the characteristic ratio is

$$S = \frac{R}{D_p} \tag{15}$$

Procedure

Each test specimen consisted of a cylinder, 6 in. long and 1.5 in. diam., with a chromel-constantan thermocouple permanently embedded along its axis. The butt-welded junction of the thermocouple was located at the geometric center of the cylinder.

First the thermocouple was mounted coaxially in a rigid paperboard tube. The constituents were mixed in specific proportions and poured into the tube. Then, after hardening, the sample was removed from the tube and connected to a yoke suspended over an agitated ice bath. The specimen was allowed to attain equilibrium at room temperature, and was then quenched in the ice bath. The electromotive force of the embedded thermocouple was recorded versus time.

Each run was repeated to establish reproducibility; all runs were found to be reproducible within 1%. Each sample was then sectioned for examination of particle distribution. This was accomplished by direct count in the granular systems and by density measurements in the tabular system. In no instance was particle settling or agglomeration observed.

TREATMENT OF DATA

The following expression predicts the temperature history on the axis of an infinitely long cylinder, which is initially at a uniform temperature T_0 and which is suddenly quenched in a fluid at 0°C.:

$$\frac{T(t)}{T_0} = 2N_{Bi} \sum_{n=1}^{\infty} \frac{e^{(-\lambda_n)^2 \frac{\alpha t}{R^2}}}{(N_{Bi}^2 + \lambda_n^2)\, J_0(\lambda_n)} \tag{16}$$

where

$$N_{Bi} = hR/k \tag{17}$$

The λ_n are roots of the characteristic equation

$$\lambda_n J_1(\lambda_n) = N_{Bi} J_0(\lambda_n) \tag{18}$$

and both α and k are assumed to be temperature independent.

The heat transfer coefficient h of Equation (17) refers to the external water film surrounding the test specimen. The value of this film coefficient was determined to be 220 B.t.u./(hr.)(sq.ft.)(°F.). This value was obtained by measuring the temperature change of water flowing through a copper coil immersed in the agitated ice bath and then back calculating to obtain the value of the external film coefficient. It is to be noted that the method of processing the data, discussed below, also yields a value of N_{Bi}, and thus h. The value of h calculated from the best values of N_{Bi} and k_{eff} was 220 B.t.u./(hr.)(sq.ft.)(°F.).

Arpaci (*20*) outlines the development of Equation (16), which is rigorous only for an infinite cylinder. However, it predicts within 0.01% the thermal behavior of a finite cylinder with an L/D of at least 4/1, as shown by comparison with exact solutions for finite cylinders (*21*). We checked this experimentally on a cylindrical test specimen provided with thermocouples for measuring the axial temperature at three points, center and 1 in. on either side of center. Within the limits of accuracy of the thermometric system employed (0.5°C.), these three temperatures were identical during the entire cooling period.

If a solid is macroscopically homogeneous and isotropic, its thermal behavior should be governed by the equations for an homogeneous solid. Therefore the raw experimental data were processed on the basis of Equations (16) and (17) plus Equation (19), which relates effective thermal conductivity to effective thermal diffusivity.

$$k_{eff} = \alpha_{eff} [\rho^I C_p{}^I (1 - \phi) + \rho^{II} C_p{}^{II} \phi] \tag{19}$$

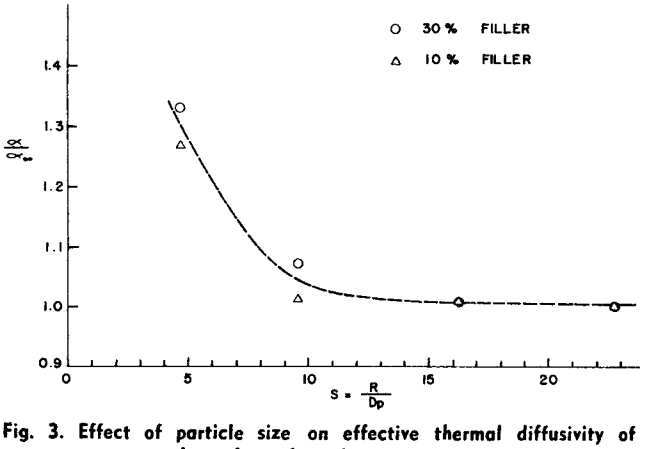

Fig. 3. Effect of particle size on effective thermal diffusivity of the carborundum-plaster system.

For each sample we found by least squares analysis that value of α_{eff} which afforded the best agreement between predicted and observed temperature versus time behavior while simultaneously satisfying Equations (17) and (19). This necessitated a trial and error procedure.

First, an initial guess of N_{Bi} was used to find α_{eff} by Equation (16). Then k_{eff} was obtained by Equation (19) and substituted into Equation (17). This provided a new estimate of N_{Bi}, and the process was repeated until no further change in N_{Bi} was observed.

A typical good fit gave an average difference of 0.1°F. between prediction and observation. In each case the infinite series was truncated after the first four terms; this partial sum produced truncation errors of less than 10^{-5}.

By analysis of Equation (16), the relative error of α_{eff} was found to be ±6.8% (*21*).

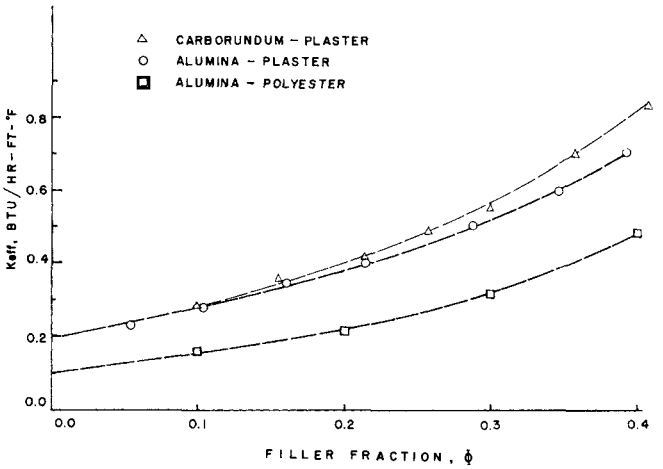

Fig. 4. Effective thermal conductivity versus filler fraction for three composite systems.

RESULTS AND DISCUSSION

Results of the particle size study are presented in Figure 3. Effective thermal diffusivities, relative to α_x, the effective diffusivity of the smallest particle size range, are plotted versus the dimensionless ratio S.

Thermal diffusivity decreases with decreasing particle size (increasing S) up to a value of S of about 10; beyond this, no further change in diffusivity occurs. Two possible explanations for this were considered: contact resistance at the matrix-filler interface, or departure from homogeneity at the larger particle sizes.

If contact resistance were significant it would tend to depress apparent thermal diffusivity. This effect would become increasingly pronounced with decreasing particle size, due to a corresponding increase in interfacial area per unit volume. Figure 3 does not show such behavior consistently; k_{eff} is essentially constant for the smaller particle sizes. Therefore contact resistance is probably not the cause of the phenomenon of Figure 3.

If a sample were not macroscopically homogeneous, one could reasonably expect poor conformance between experimental results and Equation (16), which is presumed to be a good approximation only for a macroscopically homogeneous composite. In addition, thermal diffusivity would be very sensitive to particle placement; thermal diffusivities of samples of identical composition but different particle placement would probably not be reproducible. Samples in the region of S less than 10 (large particle sizes) show both poorer conformance (0.3°F. average deviation versus 0.1°F.) and poorer reproducibility (within 15% versus within 5%) than do samples with smaller particles. Presumably, therefore, there is a plateau or break point (in our case at S = 10) below which samples are not macroscopically homogeneous, due to the size of their embedded particles.

The results of Hamilton and Crosser (*15*) apparently are in conflict with our findings. They used a composite of 27% aluminum particles of regular shapes in silicone rubber (k^{II}/k^{I} = 1,080). Their results showed no change in effective thermal conductivity for spheres with a 100-fold ratio of diameter, corresponding to S values of 6.4 and 640. Other shapes, cylinders and parallelepipeds, showed substantial increases in conductivity which correlated closely with the sphericity of the particle. These conductivities, however, do not show a regular dependence on any ratio of sample dimension to particle dimension.

The silicon carbide particles used in our study were of very irregular shape and rough texture; all size fractions, however, showed roughly the same distribution of particle shapes and thus were of essentially the same sphericity. Thus the trend shown in Figure 3 is a true particle size effect.

We cannot reconcile these differences at this time. We recommend using the sphericity correlation of Hamilton and Crosser for regular shaped particles. For irregular shaped particles of a narrow size range, we recommend using a value of $S = R/D_p = 10$ as the limit of macroscopic homogeneity, where D_p is the dimension of the intermediate screen for the designated size range.

In Figure 3 only one curve has been drawn through the data points. There may be a meaningful difference between the two sets of points, but the limited data do not justify two separate curves.

Figure 4 contains plots of thermal conductivity versus filler volume fraction for the three composite systems studied. In the granular systems only particles of the −12+16 fraction were used. The close proximity of the alumina-plaster and the carborundum-plaster curves demonstrates the insensitivity of k_{eff} to large changes in k^{II}. A five-fold increase in k^{II} causes a relatively small increase in k_{eff} over the entire range of interest of ϕ. This behavior agrees with that predicted by the expressions of Table 1 and the three-dimensional model of this work, all of which indicate that

$$\lim_{k^{II}\to\infty}\left[\frac{\partial k_{eff}}{\partial k^{II}}\right] = \lim_{\theta\to\infty}\left[\frac{1}{k^{I}}\frac{\partial k_{eff}}{\partial \theta}\right]_{k^{I}} = 0 \qquad (20)$$

In Figures 5 through 7 experimental results of the three composite systems are compared with predictions by our digital simulation and the models of Maxwell (*9*), Cheng and Vachon (*1*), and Baxley (*11*). The latter two were chosen for their being the most recent contributions in the field. The Maxwell model was chosen for its reputation as a predictor. Overall the best predictor of our experimental data is the model of Cheng and Vachon, which is slightly better than our simulation of the Jefferson unit cell. We have shown that consideration of tridirectional heat flux produces only a slight improvement over the unidirectional case (Figure 2). Thus we conclude that the assumption of cubic order, which the unit cell models employ, is more limiting than the assumption of unidirectional heat flux, used in the Cheng and Vachon model. Maxwell's model predicts thermal conductivities reasonably well at low filler fractions but deviates substantially at higher fractions, as much as 50% too low at 40% filler concentration.

Baxley's simulation predicts low values at low concentrations. Then an abrupt change of slope occurs around

30% filler. Baxley (22) attributes this to channeling, that is, a tendency for rectangular parallelepipeds to be formed by stacking of successive cubes of filler during the random placement process. Some of these filaments are oriented in the PDHT, which results in higher apparent thermal conductivities. This was confirmed by modifying Baxley's program to prevent the formation of these filaments. The effect of this was to give consistently lower effective conductivities, lower even than Maxwell's.

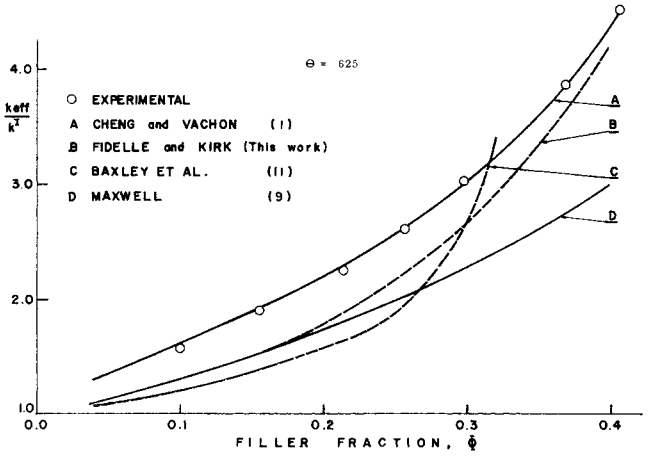

Fig. 5. Comparison of experimental results of the carborundum-plaster system with several models for predicting effective thermal conductivity.

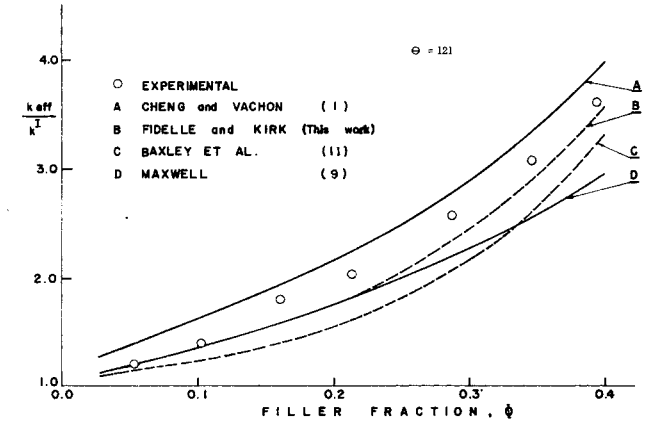

Fig. 6. Comparison of experimental results of the alumina-plaster system with several models for predicting effective thermal conductivity.

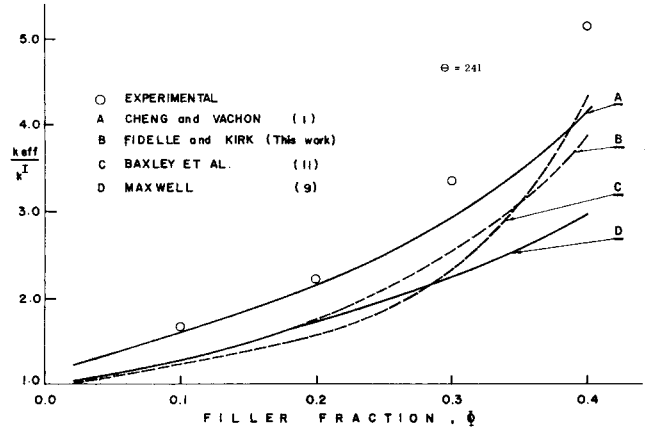

Fig. 7. Comparison of experimental results of the alumina-polyester system with several models for predicting effective thermal conductivity.

SUMMARY

From this present work, the authors conclude the following:

The assumption of unidirectional heat flux in models for predicting effective thermal conductivities of particulate composites is not a severely limiting assumption.

In a particulate composite system, the effect of a large change in the conductivity of the particulate phase, for a given continuous phase, is quite small.

Of the models examined, a recent contribution by Cheng and Vachon is the best predictor of effective thermal conductivities of composite solids.

There exists a ratio of system dimension to particle dimension below which a particulate composite can no longer be called macroscopically homogeneous. This critical ratio has a value of about 10 when the characteristic system dimension is determined from the principal direction of heat transfer and the characteristic particle dimension is determined from the size of the intermediate screen of a narrow fraction of irregular particles.

NOTATION

C_p = pure component heat capacity, B.t.u./(lb.)(°F.)
D = diameter of the test specimen, ft.
D_p = apparent particle diameter, as characterized by the sieve opening of the intermediate screen, ft.
h = heat transfer coefficient at the sample surface, B.t.u./(hr.)(sq.ft.)(°F.)
J_0 = Bessel function of the first kind, order zero
J_1 = Bessel function of the first kind, order one
k = thermal conductivity, B.t.u./(hr.)(ft.)(°F.)
L = length of the test specimen, ft.
M = width of the simulation, number of nodes per side
N_{Bi} = Biot number, dimensionless
P_1 = parameter describing concentration profile (Tsao's equation)
$\bar{q}$ = average heat flux, B.t.u./(hr.)(sq.ft.)
R = radius of the test specimen, ft.
S = characteristic ratio of system dimension to particle dimension, dimensionless
T = temperature, dimensionless
t = time, hr.
w = relaxation factor, dimensionless
x, y, z = symbols for the Cartesian coordinate system

Greek Letters

α = thermal diffusivity, sq.ft./hr.
α_∞ = thermal diffusivity of samples with smallest size particles (Figure 3)
θ = pure component thermal conductivity ratio, dimensionless
ρ = pure component density, lb./cu. ft.
τ_1 = temperature of the isothermal surface at $z = 1$
τ_2 = temperature of the isothermal surface at $z = 0$
ϕ = volume fraction of the particulate phase
μ = mean of parameter P_1
σ = variance of parameter P_1

Subscripts

eff = effective, average, or bulk property
j = j^{th} node
p = represents the six nodes surrounding the node (x, y, z)
0 = initial time

Superscripts

I = matrix or continuous phase
II = filler or disperse phase
$*$ = new policy in the iteration scheme

LITERATURE CITED

1. Cheng, S. C., and R. I. Vachon, *Intern. J. Heat Mass Transfer*, **12**, 249 (1969).
2. Gorring, R. L., and S. W. Churchill, *Chem. Eng. Progr.*, **57** (7), 53-59 (1961).
3. Woodside, W., and J. H. Messmer, *J. Appl. Phys.*, **32** (9), 1688-1706 (1961).
4. Griffis, C. L., N. C. Nahas, and J. R. Couper, *Univ. Arkansas Eng. Exp. Sta. Res. Rept. No. 5* (1964).
5. Deissler, R. G. and C. S. Eian, *NACA RM E52C05* (1952).
6. Krupiczka, R., *Intern. Chem. Eng.*, **7** (1), 122 (1967).
7. Hashin, Z., *J. Composite Materials*, **2** (3), 284 (1968).
8. Landauer, R., *J. Appl. Phys.*, **23**, 779 (1952).
9. Maxwell, J. C., "A Treatise On Electricity And Magnetism," 3rd edit., Vol. I, Chapt. 9, Art. 314, Dover, New York (1954).
10. Dul'nev, G. N., *Inz-Fiz. Zh.*, **9**, (3), 399 (1965).
11. Baxley, A. L., N. C. Nahas, and J. R. Couper, in "Proceedings of The Seventh Conference on Thermal Conductivity," Natl. Bur. Standards Special Publ. No. 302, 685-694 (Sept. 1968).
12. Tsao, G. T., *Ind. Eng. Chem.*, **53**, (5), 395 (1961).
13. Warren, J. E., and J. H. Messmer, *Ind. Eng. Chem. Fundamentals*, **1** (3), 222,223 (1962).
14. Nielson, L. E., *J. Composite Materials*, **1** (2), 100 (1967).
15. Hamilton, R. L., and O. K. Crosser, *Ind. Eng. Chem. Fundamentals*, **1** (3), 187 (1962).
16. Springer, G. S., and S. W. Tsai, *J. Composite Materials*, **1** (2), 166 (1967).
17. Thornburgh, J. D., and C. D. Pears, *A.S.M.E. Publ. 65-WA/HT-4*, (1965).
18. Jefferson, T. B., O. W. Witzell, and W. L. Sibbitt, *Ind. Eng. Chem.*, **50** (10), 1589-1592 (1958).
19. Jakob, M., "Heat Transfer," Vol. I, p. 88, Wiley, New York (1950).
20. Arpaci, V., "Conduction Heat Transfer," p. 284, Addison-Wesley, Reading, Mass. (1966).
21. Fidelle, T. P., Ph.D. dissertation, Univ. Massachusetts, Amherst (1969).
22. Baxley, A. L., and J. R. Couper, *Univ. Arkansas Eng. Exp. Sta. Res. Rept. No. 8* (1966).
23. Goldsmith, A., et al., "Handbook of Thermophysical Properties of Solid Materials," Macmillan, New York (1961).

Manuscript received June 17, 1970; revision received February 9, 1971; paper accepted February 10, 1971.

Experimental Evaluation of Dynamic Models for a Fixed-Bed Catalytic Reactor

J. A. HOIBERG, B. C. LYCHE, and A. S. FOSS

Department of Chemical Engineering

University of California, Berkeley, California

Experimental observations of a reactor's frequency response when compared with mathematical models of the reactor revealed the need for accurate modeling of heat generation, heat exchange, and heat storage processes. The experiments were performed in a laboratory reactor with the exothermic reaction between hydrogen and oxygen catalyzed by platinum on granules of silica gel. This system permitted observation of several nonlinear effects.

One- and two-dimensional, locally linear, plug-flow models of the continuum type were used for the comparison. One of the models included the effects of intraparticle diffusion of reactants. However, models that neglected intraparticle dynamic effects were found suitable here because the decay time for the diffusion process within the catalyst was short compared to the reactor's major thermal time constant. A two-dimensional model was found to give an excellent representation of the very complex movement of concentration and temperature waves in this type of reactor, while a one-dimensional model was found to serve well when radial gradients are small.

Although many different types of mathematical models of fixed-bed reactors have been in use for several decades, there still remain a number of uncertainties regarding the amount of detail needed in models of the dynamic behavior of these reactors. The catalytic fixed-bed reactor with gaseous reactants, the type of system treated here, is particularly rich in these uncertainties. For example, the generation, transport, and storage of heat are processes of prime importance in this type of reactor, but the detail with which these processes must be represented in dynamic models is not at all certain, and indeed varies from case to case. The misjudgment of this detail may lead, on the one hand, to a model incapable of representing the principal behavior and, on the other, to a model that is computationally and analytically intractable.

These concerns have prompted this experimental investigation of the importance and influence of the numerous physical and physicochemical phenomena active under dynamic conditions. A fixed-bed reactor in which the highly exothermic reaction between hydrogen and oxygen occurred on a platinum catalyst was subjected to sinusoidal disturbances in the feed temperature and feed composition. Shown here is a comparison of the intricate behavior of the resulting temperature and concentration

J. A. Hoiberg is at Continental Oil Company, Ponca City, Oklahoma 74601. B. C. Lyche is with Dow Chemical Company, Terneuzen, The Netherlands.